Journal of Catalysis 420 (2023) 99–109

Contents lists available at ScienceDirect

Journal of Catalysis

journal homepage: www.elsevier.com/locate/jcat

Particle size dependence of ethylene epoxidation rates on Ag/α-Al_2O_3 catalysts: Why particle size distributions matter

Krishna R. Iyer, Aditya Bhan *

Department of Chemical Engineering and Materials Science, University of Minnesota, Minneapolis, MN 55455, USA

ARTICLE INFO

Article history:
Received 18 November 2022
Revised 30 January 2023
Accepted 11 February 2023
Available online 16 February 2023

Keywords:
Ethylene epoxidation
Particle size distribution
Promoters
Alumina
Silver

ABSTRACT

The post-reaction Ag surface area distribution of 16 Ag/α-Al_2O_3 ethylene epoxidation catalysts with varying Ag weight loadings (6.9 – 35 wt%) containing different distributions of Ag particle sizes was correlated with measured ethylene oxide (EO) rates in presence of 3.5 ppm ethyl chloride via a particle size dependent Gaussian rate function. The Gaussian rate function model differs from a description based on average particle size as it accounts for the effects of the breadth of particle size distribution as well as the population of different particle sizes that constitute the Ag particle distribution on measured EO rates. This description of particle size effects in ethylene epoxidation catalysis facilitates accurate prediction of EO rates over a wide range of particle sizes (5–400 nm) and suggests that very small (5–50 nm) and very large Ag particles (>250 nm) have low EO rates (<3 μmol g_{Ag}^{-1} s^{-1}). A narrow Ag particle size distribution centered around ~130–150 nm would enable operation of ethylene epoxidation with high EO rates and EO selectivity.

1. Introduction

Identification and quantification of active sites relating structure and morphology of a catalyst formulation to its rate is a key objective in catalysis. Metal nanoparticles supported on a porous non-metallic support are a class of catalysts wherein typically the exposed metal atoms constitute the active site. Certain reaction systems [1–4] exhibit a particle size effect wherein the rate of the catalytic event sensitively depends on changes in the coordination and electronic environment induced by aggregation and clustering of metal atoms which in turn changes the ability of the catalytic center to adsorb or desorb catalytically relevant species. The two macroscopic observables relevant for developing structure–function correlations in such systems are the metal particle size distribution and the rate. For convenience and by convention, the particle size distribution is only represented by a single number—the average particle size, without explicitly accounting for any other characteristics of the distribution.

Selective chemisorption, scanning and transmission electron microscopy, X-ray diffraction, among other methods are used to measure metal particle sizes however, only an average particle size is reported when in practice there is a broad distribution of particle sizes. We demonstrate for ethylene epoxidation over Ag/α-Al_2O_3 catalysts that this representation of the particle size distribution with an average particle size, while simple and convenient, and almost universally adopted, is insufficient to explain the particle size dependence of measured epoxidation rates. Consider a scenario in which two catalyst samples have the same average particle size albeit resulting from very different particle size distributions. Lumping all description of the particle size distribution into a single average measure masks the contributions from metal clusters of different sizes which may contribute differently to the observed reaction rate.

The effects of Ag particle size on ethylene epoxidation rates and ethylene oxide (EO) selectivity over Ag/α-Al_2O_3 catalysts have been extensively investigated previously [5–14]. Van Der Reijen et al. [5] measured ethylene oxidation rates (0.1–1.5 μmol C_2H_4 $g_{Ag\ exposed}^{-1}$ s^{-1}) over a series of 18 wt% Ag/α-Al_2O_3 catalysts, treated under different gas environments and temperatures, at 473 K and 1 bar pressure (30 mol% C_2H_4, 8.5 mol% O_2) and found that EO rates increase with increasing surface area averaged Ag particle size up to 60 nm and thereafter decrease with Ag particle size. Similarly, an optimum in ethylene oxidation rates with mean Ag crystallite size was observed by Lee et al. [6] over 2–10 wt% Ag/α-Al_2O_3 catalysts at 503 K and 13 bar pressure (3 mol% C_2H_4, 12 mol% O_2) and by Goncharova et al. [7] over 0.5–13 wt% Ag/α-Al_2O_3 catalysts at 500 K and 1 bar (2 mol% C_2H_4, 7 mol% O_2). Contrary trends were observed by Van hoof et al. [8] wherein EO rates decrease with increasing average particle size until 50 nm before becoming

* Corresponding author.
E-mail addresses: iyer0040@umn.edu (K.R. Iyer), abhan@umn.edu (A. Bhan).

https://doi.org/10.1016/j.jcat.2023.02.008
0021-9517/

constant with size over 1–14 wt% Ag/α-Al_2O_3 catalysts at 498 K and 20 bar (5 mol% C_2H_4, 10 mol% O_2) both in presence and in absence of 1 ppm vinyl chloride. Other studies allude to the effects of Ag particle size on EO selectivity. Christopher and Linic [9] measured ethylene epoxidation rates over Ag/α-Al_2O_3 catalysts having different shapes (nanospheres, nanocubes, and nanowires) and sizes (75 nm to 350 nm) at 510 K and 1 atm pressure (10 mol% C_2H_4, 10 mol% O_2) and observed that EO selectivity increased with increasing particle size and oxygen partial pressure. At identical reaction conditions, large (350 nm) nanocube-shaped catalysts, terminated by Ag (100) surface facets ascertained using HRTEM imaging, offered the highest EO selectivity among the different shapes and sizes tested. Egelske et al. [10] also tested several 0.3–5 wt% Ag/α-Al_2O_3 catalysts at 483 K and 17 bar pressure (25 mol% C_2H_4, 8 mol% O_2) and observed an increase in EO selectivity from 58% for an average particle size of 65 nm to 75% at 350 nm. A summary of the catalyst specifications and the reaction conditions employed in previous studies examining particle size effects in ethylene epoxidation is given in Table 1. The disparity in the observed EO rates with particle size among different studies is plausibly due to some differences in catalyst formulation and differences in some process conditions including use of C_2H_4 or O_2 rich reactant mixtures, presence/absence of chlorine, total pressure, and temperature. What is noteworthy is that trends in EO rates differ from one study to another when using average size as a descriptor. We inquire whether these distinctions arise because particle sizes are assessed merely by the mean of the distribution not accounting for the broad distribution of Ag particle sizes.

Several authors have noted previously that Ag undergoes restructuring [15,16] and sintering [17,18] during ethylene epoxidation. Van Hoof et al. [15] carried out STEM imaging of an 8.1 wt% Ag/α-Al_2O_3 catalyst before and after reaction (20 bar, 498 K, 5 mol% C_2H_4, 10 mol% O_2) and found that the average Ag particle size increased from 107 nm to 119 nm in presence of 1 ppm vinyl chloride in the reactor feed. Particle size distributions measured after reaction thus are likely more representative of the operational state of the epoxidation catalyst and as such these distributions should be correlated with epoxidation rates.

Weber, in a recent publication [19], articulated the limitations of using fractional metal exposure as a measure of active sites in a catalyst because it obscures the distribution of active sites. In making this point, Weber considered 5–30 wt% Pt/C catalysts with mean crystallite sizes between 1 and 4 nm synthesized by Peukert et al. [20] to have a particle size distribution that can be represented by: (i) a Rayleigh distribution with the same mean particle size, with some variance in the distribution, or (ii) a Delta function centered at the mean particle size not accounting for the distribution of particle sizes. Weber assumed that a subset of sites with a specific configuration (C9 sites in this example) are the relevant active sites whose population can be represented by a distribution that varies with particle size in a power law manner. The particle size dependency of measured turnover rates was captured only by expressing the rate as a continuous function of particle size (integral of the population of C9 sites at a particular particle size 'r' multiplied by the population of particles of size 'r') and by considering the distribution of particle sizes (Rayleigh distribution in this example), presenting a hypothetical example of correlating the particle size distribution with measured rates.

In this study, we develop a particle size dependent rate function model that allows us to map changes in the Ag particle size distribution to observed changes in EO rates. We measured ethylene epoxidation rates over 13 different Ag/α-Al_2O_3 catalysts with 6.9–35wt.% Ag weight loadings and 3 other formulations obtained by physically mixing two catalyst formulations, such that the 16 samples have a wide range of Ag particle sizes (5–400 nm). The

Table 1
Catalyst specifications and reactions conditions for previous studies on particle size effects in ethylene epoxidation on Ag-based catalysts.

Reference	Catalyst	Average particle size range	C_2H_4: O_2 ratio in the reactor feed	Total pressure and temperature	Chlorine promoters	Observations
Wu and Harriott (11)	(1–11 g) 0.5–39.5 wt% Ag/SiO_2	5–50 nm	1:1	1.3 bar, 493 K	none	EO rates increase until 12 nm and then decrease and EO selectivity increases with Ag crystallite size
Verykios et al. (12)	(1–11 g) 1–14 wt% Ag/α-Al_2O_3	30–180 nm	1:5	1.3 bar, 493 K	none	EO rates decrease from 30 to 50 nm before increasing continuously with size whereas EO selectivity increases until 130 nm before decreasing with Ag crystallite size
Cheng and Clearfield (13)	(0.5 g) 3–55 wt% Ag/Zr $(NaPO_4)_2$	5–85 nm	1:15	1 bar, 503 K	none	EO rates and EO selectivity increase until 27 nm before decreasing continuously with size
Lee et al. (6)	0.5–10 wt% Ag/α-Al_2O_3	20–100 nm	1:4	0.1 bar, 508 K	none	EO rates increase until 40 nm and then decrease with Ag crystallite size whereas EO selectivity increases until 60 nm, and then becomes invariant with size
Goncharova et al. (7)	(0.5–2 g) 0.5–13 wt% Ag/α-Al_2O_3	20–100 nm	1:3.5	1 bar, 503 K	none	EO rates increase until 60 nm and then become invariant with size whereas EO selectivity increases with size
Lu et al. (14)	(0.5 g) 0.5–56 wt% Ag/$CaCO_3$	50–370 nm	1:1.7	3 bar, 475 K	none	Turnover frequencies for ethylene consumption and EO selectivity increase with size
Van den Reijen et al. (5)	(0.15 g) 18 wt% Ag/α-Al_2O_3	20–500 nm	3.5:1	1 bar, 473 K	none	EO rates increase until 60 nm and then decrease and EO selectivity is invariant with Ag particle size
Van Hoof et al. (8)	(0.02–0.15 g) 1.3–14.4 wt% Ag/α-Al_2O_3	19–300 nm	1:2	20 bar, 498 K	None or 1 ppm vinyl chloride	EO rates decrease with average particle size until 50 nm before becoming constant with size whereas EO selectivity increases with size
Egelske et al. (10)	0.3–5 wt% Ag/α-Al_2O_3	65–350 nm	3.1:1	17 bar, 483 K	none	Turnover frequencies for ethylene consumption and EO selectivity increase with size

exposed surface area of Ag particles post-reaction for each of the 16 catalyst formulations was observed to follow a lognormal distribution. Epoxidation rates on these 16 samples were measured in presence of an organochloride promoter (3.5 ppm C_2H_5Cl) and these samples exhibited nearly invariant EO selectivity (~75–81%). We represent the measured EO rates as a continuum i.e., as an integral of the product of a Gaussian rate function and the lognormal surface area distribution to capture the contributions of different particle sizes to the rate eschewing any assumptions of site ensemble requirements or specificity of a particular Ag crystal facet or site. The rate-function model results in an explicit description of the Ag particle size distribution and the rate dependence on Ag particle size. The model captures the low reactivity of very small Ag particles (5–50 nm) and very large Ag particles (>250 nm) and leads us to postulate that a narrow Ag particle size distribution centered around 130-150 nm will facilitate high EO rates and EO selectivity over Ag/α-Al_2O_3 catalysts.

2. Materials and methods

2.1. Catalyst synthesis

The Ag/α-Al_2O_3 formulations in this report were synthesized by incipient-wetness impregnation of a silver oxalate ($Ag_2C_2O_4$) precursor over α-Al_2O_3 following protocols established previously by several authors [5,8,21]. Catalox HPa-150 γ-Al_2O_3 was heat treated in stagnant air at 1698 K for 4 h with a ramp rate of 0.033 K s^{-1} to synthesize the α-Al_2O_3 support. $Ag_2C_2O_4$ was synthesized as a precipitate by mixing a 0.24 M solution of oxalic acid (oxalic acid dihydrate, Fisher Scientific, 99.6%) in HPLC-grade water with an equimolar amount of silver nitrate (Thermo Scientific, 99.7%) at ambient temperature. The $Ag_2C_2O_4$ precipitate was washed three times in HPLC-grade water before filtration under vacuum for ~12 h at ambient temperature. A solution containing 1:3 M ratio of silver oxalate: ethylene diamine (Sigma-Aldrich, Reagent-Plus, >99%) diluted in 2 cm^3 HPLC-grade water was impregnated onto the α-Al_2O_3 support before drying in static air at 333 K. The molarity of $Ag_2C_2O_4$ solution was varied between 0.5 M and 2.5 M to obtain Ag/α-Al_2O_3 catalysts with different Ag weight loadings from 6.9 to 35% as confirmed using SEM-EDX analysis. Upon drying, the Ag-impregnated support was treated in 0.83 cm^3 s^{-1} flow of pure He (Research grade) at 498 K for 2 h to breakdown the Ag precursor and form Ag/α-Al_2O_3. The catalyst (1 g) was heat treated post synthesis under different gas atmospheres (H_2 (Airgas, UHP 99.999%), He (Matheson, Research grade), zero-grade air, and O_2 (Matheson, 99.9%)) at flowrates of 0.8–1.25 cm^3 s^{-1} and temperatures between 498 and 943 K to obtain a wide range of Ag particle sizes derived from procedures previously detailed by Van der Reijen et al. [5] The heat treatment conditions used to modify Ag particle sizes are detailed in Table 2 (Section 3.1).

2.2. Catalyst characterization

The crystalline phases in Ag/α-Al_2O_3 samples were determined by powder X-ray diffraction (p-XRD) using Cu K_α radiation (λ = 0.154 nm) on a Bruker-AXS (Siemens) D5005 diffractometer (Supporting Information Section S.1). Ag nanoparticle size was measured after reaction by Scanning Electron Microscopy (SEM, JEOL 6500 Field Emission gun, 10 kV electron beam accelerating voltage). The spent catalyst was prepared for SEM imaging by coating it on a thin film of amorphous carbon. Three SEM images representing different regions over the catalyst and ~1600 Ag particles were analyzed for each catalyst sample using ImageJ to evaluate the Ag particle size distribution (Supporting information Figure S.2). The sampling error made in representing the population of total Ag particles with a sample of size 1600 was quantified to be <1% (Supporting Information Section S.2).

2.3. Measurement of steady state rates of ethylene epoxidation

Rates of ethylene epoxidation were measured in a stainless-steel packed-bed reactor (McMaster- Carr, OD = 6.36 mm, ID = 4.57 mm), containing 25–100 mg of Ag/α-Al_2O_3 catalyst loaded between two plugs of quartz wool (CE Elantech). The reactor was held between two split-tube copper sleeves and heated by two cartridge heaters (Omega Engineering Inc., CIR-2100, 600 W) with heating controlled using a Watlow temperature controller (96 Series) and pressure maintained at 530 kPa using a backpressure regulator (Tescom). The reaction temperature (513 K) was measured using a K-type thermocouple (Omega Engineering Inc.) placed in the center of the catalyst bed. The reactor feed consisted of 30 mol% C_2H_4 (Airgas 99.99%), 0.4 mol% C_2H_6 (Matheson 10% diluted in He), 7.7 mol% O_2 (Matheson 99.99%), 3.5 ppm C_2H_5Cl (Airgas 160 ppm diluted in He), and 1 mol% CO_2 (Matheson 10% diluted in He), was unchanged for all ethylene oxidation experiments and the respective gases were supplied to the reactor through mass flow controllers (MKS G-series) at a total flowrate of 2.78 cm^3 s^{-1}. At the process conditions, the measured EO rates were free from external heat and mass-transfer limitations as confirmed by the invariance of EO rates with space velocity (Supporting Information Figure S.3) as well as calculations using GradientCheck [22] reported in Section S.3 of the Supporting Information. The reactor effluent composition was analyzed using a gas chromatograph (GC, Agilent 7890A) equipped with an HP-Plot Q column (30 m × 320 μm × 20 μm) and a thermal conductivity detector (TCD) in series with a flame ionization detector (FID) before the effluent was discharged into a bubbler containing 0.5 M H_2SO_4 (BeanTown Chemical). The gas lines upstream of the reactor were maintained above 393 K using heat tapes (W.W. Grainger) to prevent condensation of the effluent gas stream. Ethylene conversions varied between 0.2 and 0.7% and oxygen conversions were <5% for all data reported, and the carbon mass balance (total carbon moles in/total carbon moles out) closed within 2%. Product selectivities reported in the study are defined as moles of carbon in the product divided by moles of carbon in all products. Major reaction products include EO, CO_2, and H_2O with trace amounts of acetaldehyde formed (<1% selectivity). Steady-state rates reported in this study are determined after exposing the catalyst to the reaction mixture for 18 h to allow for the slow evolution of the catalyst with time on-stream (Supporting Information Figure S.5).

3. Results and discussion

3.1. Analysis of Ag particle size distribution

The Ag particle size distribution of Ag/Al_2O_3 catalysts with different Ag weight loadings was varied using heat treatments under different gas environments ($He/H_2/O_2$). An increase in the average Ag particle size of the Ag/α-Al_2O_3 catalyst after attaining steady state rates compared to that of the as-synthesized sample (Supporting information Figure S.6) is consistent with observations made previously by several authors noting Ag undergoes restructuring [15,16] and sintering [17,18] during ethylene epoxidation; therefore, we determined particle size distribution of Ag/α-Al_2O_3 catalysts after reaction. A summary of total surface area per gram, surface area weighted particle diameter ($D_{S.A.}$), and heat treatment conditions used to modify the particle size distribution of all the catalysts and physical mixtures of catalysts is given in Tables 2 and 3 respectively. A comparison of average diameters and surface

Table 2
Surface area weighted particle diameter ($D_{S.A.}$), total surface area per gram, and heat treatment conditions employed for different Ag/α-Al_2O_3 catalysts. The Ag weight loading of the sample has been mentioned as a prefix in the sample name. All catalysts were initially treated in 1.25 $cm^3\ s^{-1}$ flowing He at 498 K with a ramp rate of 0.17 K s^{-1} and dwell time of 2 h except 31S-9 which was treated in 1.25 $cm^3\ s^{-1}$ flowing H_2 at 498 K. Histograms depicting the surface area per gram as a function of particle size for all catalysts are shown in Supporting Information Section S.9.

Sample name	$D_{S.A.}$ / nm	Total area per gram / $m^2_{Ag}g^{-1}_{Ag}$	Heat treatment conditions
6.9S-1	69.4 ± 23.4	8.0	1.25 $cm^3\ s^{-1}$ H_2, ramp at 0.17 K s^{-1}, hold at 498 K for 4 h
9.9S-2[1]	74.6 ± 25.4	6.4	–
16.9S-2[1]	93.6 ± 31.5	5.4	–
16.9S-1	101.7 ± 33.1	5.8	1.25 $cm^3\ s^{-1}$ H_2, ramp at 0.17 K s^{-1}, hold at 498 K for 4 h
31S-9	151.5 ± 47.3	3.2	1.10 $cm^3\ s^{-1}$ H_2, ramp at 0.17 K s^{-1}, hold at 673 K for 4 h
35S-1	164.9 ± 50.7	3.6	1.25 $cm^3\ s^{-1}$ H_2, ramp at 0.17 K s^{-1}, hold at 498 K for 4 h
35S-2[1]	176.1 ± 54.1	3.2	–
35S-3	181.7 ± 57.4	2.7	0.83 $cm^3\ s^{-1}$ He, ramp at 0.17 K s^{-1}, hold at 773 K for 4 h
35S-4	203.4 ± 70.3	2.4	0.83 $cm^3\ s^{-1}$ air, ramp at 0.17 K s^{-1}, hold at 598 K for 4 h
35S-5	257.7 ± 75.2	2.0	0.83 $cm^3\ s^{-1}$ O_2, ramp at 0.17 K s^{-1}, hold at 943 K for 4 h
35S-6	261.6 ± 82.6	2.1	0.83 $cm^3\ s^{-1}$ air, ramp at 0.17 K s^{-1}, hold at 848 K for 4 h
35S-7	268.1 ± 88.6	2.1	0.83 $cm^3\ s^{-1}$ O_2, ramp at 0.17 K s^{-1}, hold at 898 K for 4 h
35S-8	272.5 ± 89.3	2.1	0.83 $cm^3\ s^{-1}$ O_2, ramp at 0.17 K s^{-1}, hold at 928 K for 4 h

[1]These samples were not subjected to any additional heat treatment.

area histograms for 35S-1 and 35S-2 (Table 2 and Supporting Information Figures S.10, S.11) shows that H_2 treatment favors formation of smaller Ag particles whereas treatment in O_2 flow leads to larger Ag particles (see samples 35S-2 with 35S-7 in Table 2 and Supporting Information Figures S.11, S.16).

A typical SEM image and a histogram depicting the Ag particle size distribution of one of the Ag/α-Al_2O_3 samples are shown in Fig. 1 (a, b).

The particle size distribution can be expressed as a histogram of exposed surface area of Ag particles using Eq.1 where 's_i' is the diameter of particle 'i', n is the total number of particles, and 'ρ_{Ag}' is the bulk density of silver. The discrete surface area histogram was fitted to a continuous lognormal distribution as it captured the tail of the distribution better compared to the symmetric Gaussian distribution (Fig. 2 (a, b)). The lognormal distributions fitted to the surface area histograms for all 16 catalysts enlisted in Tables 2 and 3 are shown in Supporting Information Section S.8 along with respective SEM images for each sample (Figures S.10-S.25).

Table 3
Surface area weighted particle diameter ($D_{S.A.}$), total surface area per gram, and mixture composition for physical mixtures of Ag/α-Al_2O_3 catalysts.

Sample name	$D_{S.A.}$ / nm	Total area per gram / $m^2_{Ag}g^{-1}_{Ag}$	Mixture composition
mix-1	144.4 ± 47.8	3.9	30 wt% 35S-2 and 70 wt % 16.9S-2
mix-2	181.6 ± 59.4	2.7	40 wt% 35S-4 and 60 wt % 9.9S-2
mix-3	209.4 ± 67.4	2.3	30 wt% 35S-2 and 70 wt % 35S-5

$$\text{Surface area per gram } (m^2 g_{Ag}^{-1}) = \frac{\sum_{i=1}^{n(\text{size interval})} 2\pi\left(\frac{s_i}{2}\right)^2}{\sum_{i=1}^{n} \frac{2\pi}{3}\left(\frac{s_i}{2}\right)^3 * \rho_{Ag}} \quad (1)$$

3.2. Ethylene epoxidation rates and EO selectivity as a function of average particle size

EO rates measured at identical process conditions over 13 different Ag/α-Al_2O_3 catalyst formulations and 3 physical mixtures are shown in Fig. 3 (a). The measured rates of ethylene consumption (0.8–8 μmol $g_{Ag}^{-1}\ s^{-1}$) are comparable to rates measured by Van der Reijen et al. [5] over 18% Ag/α-Al_2O_3 at 473 K and 1 bar total pressure while they are lower than 50–100 ethylene μmol converted $g_{Ag}^{-1}\ s^{-1}$ measured by Van Hoof et al. [8] over 2–10% Ag/α-Al_2O_3 at 498 K and 20 bar total pressure plausibly because of higher total pressure. EO rates increase with increasing surface area averaged Ag particle ($D_{S.A.}$) size up to ~110 nm before starting to decrease with Ag particle size. EO selectivity, on the other hand, varied between 75 and 81% and showed no trends with average particle size (Fig. 3 (b)).

First, we considered the possibility that all Ag particles of different sizes have equal reactivity and Ag particles of different sizes contribute to rate differently only because of a difference in the surface area per gram of silver exposed by these particles. EO rates normalized by the total surface area per gram for different catalysts should collapse to a constant value if all Ag particles of different sizes have equal reactivity. Surface area normalized EO rates (EO rate / total Ag surface area per gram), calculated using rates from Fig. 3.1 (a) and the total surface area per gram from Tables 2 and 3, for all catalysts tested show ~4× variation (Fig. 4) suggesting that particles of different sizes have inherently different reactivity and thus uniquely contribute to cumulative EO rate.

We then examined the possibility that there exists a functional relationship between EO rate and average Ag particle size and this relationship is robust to describe particle size effects in ethylene epoxidation. The dependence of EO rates on the surface area-averaged particle size ($D_{S.A.}$) for the 16 samples tested can be fitted using a lognormal equation (Eq. (2)) as shown in Fig. 5. This model, if appropriate, should be able to predict the rate of a physical mixture (mix-1 in Table 3) of 16.9S-2 and 35S-2 with a $D_{S.A.}$ = 144.4 nm. EO rate predicted for mix-1 by Eq. (2) is 4.17 μmol $g_{Ag}^{-1}\ s^{-1}$ which is ~1.5× higher than the experimentally measured rate of 2.97 μmol $g_{Ag}^{-1}\ s^{-1}$ suggesting that average particle size may not be adequate as a descriptor of the size distribution of the Ag/α-Al_2O_3 catalyst. Subsequently, we attempted to map changes in Ag particle size distribution to epoxidation rates instead of using the average diameter which does not capture the variance of the distribution.

$$\text{rate}(\mu\text{mol } g_{Ag}^{-1}\ s^{-1}) = 0.39 + \frac{518.87}{\sqrt{2\pi} \times 0.36 \times D_{S.A.}} \times e^{-\frac{\left(\ln\left(\frac{D_{S.A.}}{129.68}\right)\right)^2}{2\times 0.36^2}} \quad (2)$$

3.3. Mapping the particle size distribution to EO rates using rate functions

To incorporate the Ag particle size dependence of epoxidation rates we formulated a model based on the concept proposed by Weber [19] wherein the observed rate is a cumulative quantity that reflects accrual of contributions from Ag particles of different size. Mathematically, rate is described as an integral (Eq. (3)) of the product of two terms: (i) a rate function r(s) that gives the contribution of a particle of size 's' to the EO rate and (ii) A(s) which is the surface area exposed per gram (Eq. (1)) of particles of diameter 's', evaluated across the particle size range (R_{min} to R_{max}). The surface area exposed per gram, A(s), for all catalysts is fitted by a lognor-

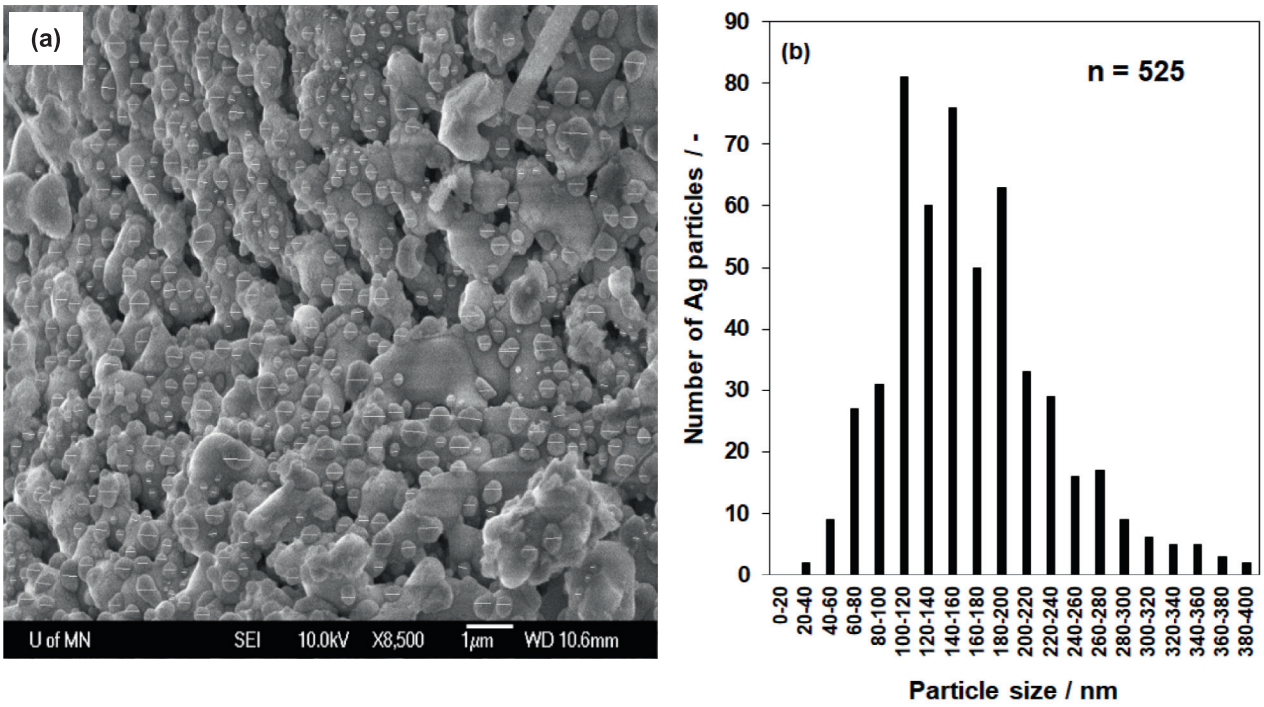

Fig. 1. (a) Representative SEM image of sample 35S-4 (refer to Table 2). (b) Measured particle diameter count distribution for a sample of 525 Ag particles. 18 h steady state reaction conditions: 30 mol% C_2H_4, 7.7 mol% O_2, 1 mol% CO_2, 3.5 ppm C_2H_5Cl, 0.4 mol% C_2H_6, balance He; 5.3 bar; 513 K; catalyst mass = 0.034 g 35S-4.

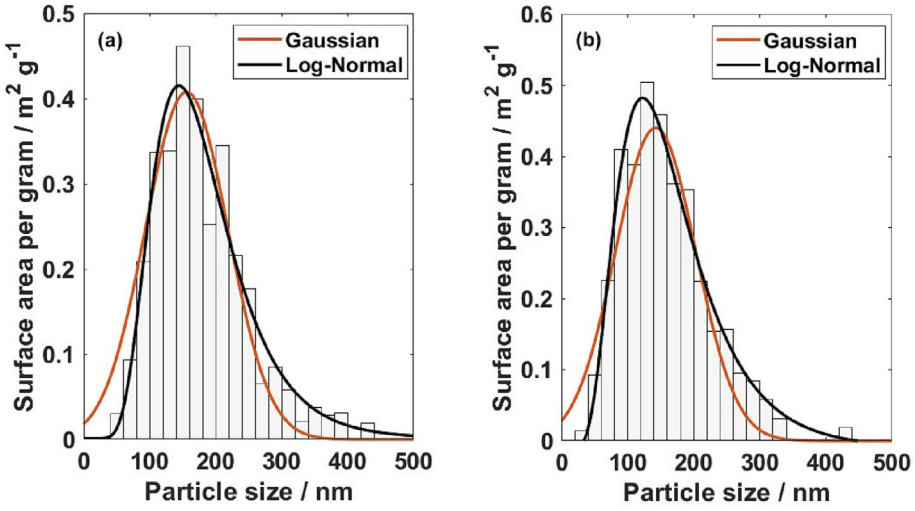

Fig. 2. A histogram of exposed surface area per gram as a function of particle size for two catalyst samples (a) 35S-2 (refer to Table 2) and (b) 35S-1 (refer to Table 2) fitted to Gaussian and lognormal distributions.

mal distribution (Eq. (5)) with A, μ, σ as its parameters (Fitted lognormal distribution functions for all catalysts are shown in Supporting Information Section S.9).

$$\text{rate}(\mu\text{mol } g_{Ag}^{-1}\ s^{-1}) = \int_{R_{min}}^{R_{max}} r(s) * (A(s))ds \tag{3}$$

$$r(s) = ae^{-\left(\frac{s+b}{c}\right)^2} \tag{4}$$

$$A(s) = \frac{A}{\sigma\sqrt{2\pi}s} e^{-\frac{(\log(\frac{s}{\mu}))^2}{2*\sigma^2}} \tag{5}$$

The epoxidation rates and the surface area per gram fitted with a lognormal distribution (Eq. (5)) across 23 data points (includes replicates and physical mixtures of catalysts) were fitted to Eq. (3) using Athena Visual Studio to find the optimal rate function parameters for r(s). The function r(s) is unknown therefore, we evaluated different functional forms: power law, polynomials, and Gaussian for the rate function r(s) and used model discrimination statistics to obtain the best fit model (detailed statistics in Supporting Information Section S.6). A Gaussian rate function model (Eq. (4)) correlates the lognormal surface area distribution to measured epoxidation rates (Fig. 6 (a)) across a wide range of Ag particle sizes (5–400 nm) evidenced by the close agreement between the measured rates and the rates predicted by the Gaus-

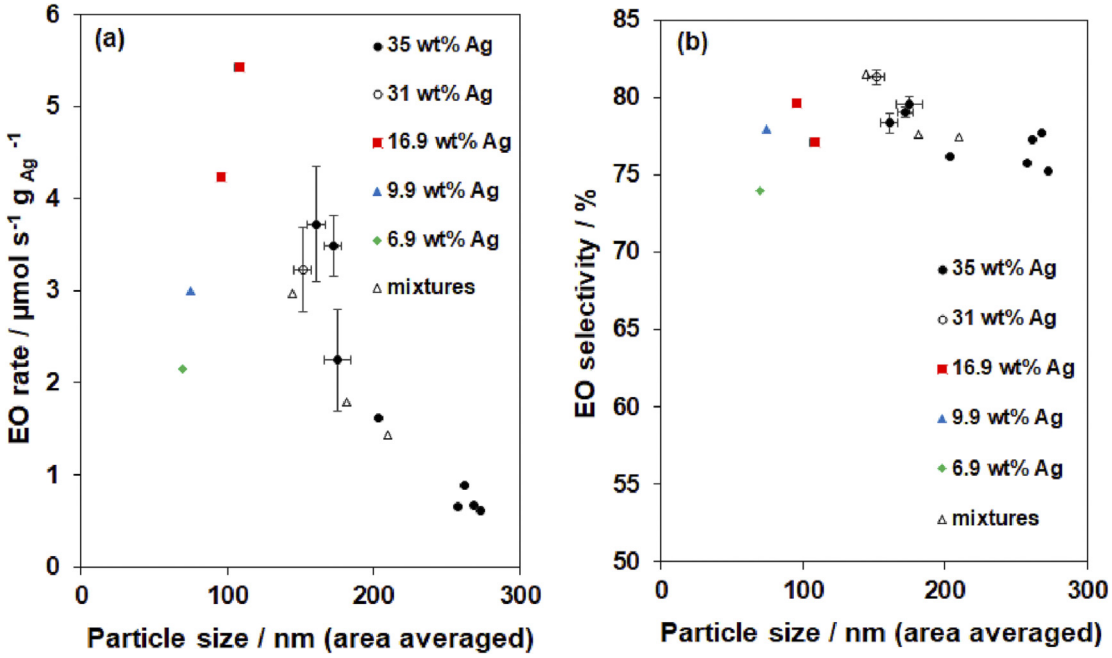

Fig. 3. (a) EO rates (b) EO selectivity measured as a function of surface area averaged particle size. Reaction conditions: 30 mol% C_2H_4, 7.7 mol% O_2, 1 mol% CO_2, 3.5 ppm C_2H_5Cl, 0.4 mol% C_2H_6, balance He; 5.3 bar; 513 K; catalyst mass = 0.027–0.082 g 6.9–35 wt% unpromoted Ag/α-Al_2O_3. Data acquired at 18 h on-stream after steady state rates were obtained.

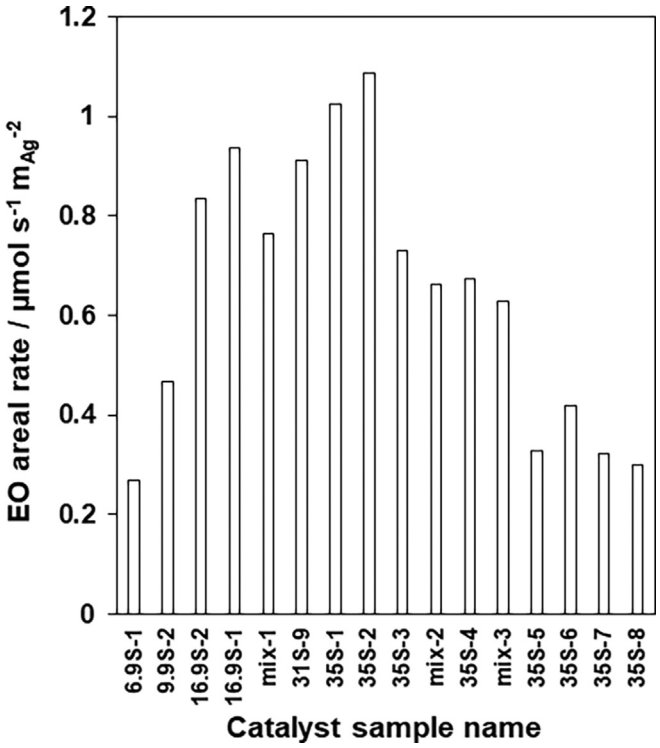

Fig. 4. Surface area normalized EO rates plotted for all the catalysts tested. Catalyst nomenclature follows the presentation in Tables 2 and 3.

sian rate function model (Fig. 6 (b)). The optimal rate function parameters for the Gaussian rate function are listed in Table 4. A more detailed discussion on the magnitude of errors in the measured EO rates and particle size distributions as well as model parameter uncertainties is given in the Supporting Information Section S.7. A residual plot displaying the deviation of the EO rate predicted by the Gaussian model from the experimental value (% residual) for all catalysts (Supporting Information Figure S.9)

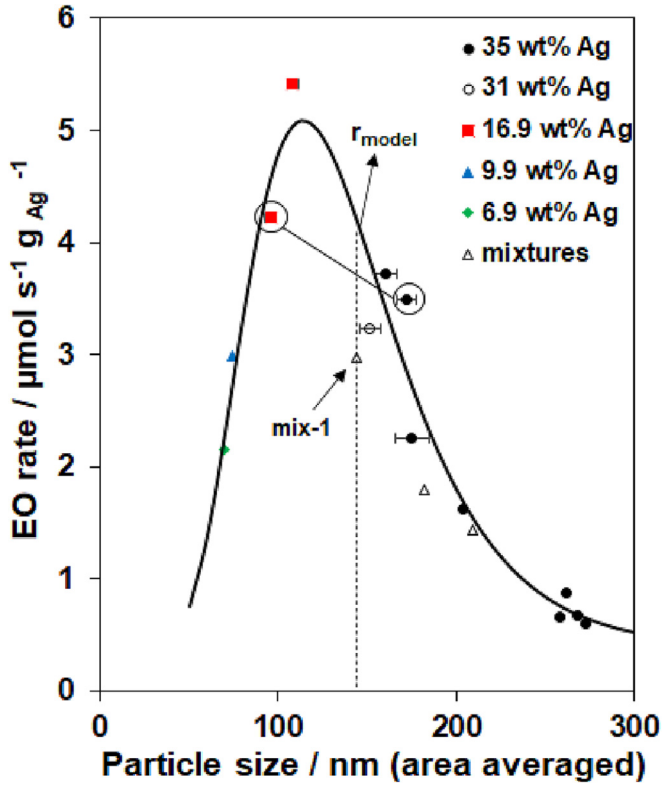

Fig. 5. EO rates measured as a function of surface area averaged particle size. The solid line is a lognormal fit according to Eq.2. Reaction conditions: 30 mol% C_2H_4, 7.7 mol% O_2, 1 mol% CO_2, 3.5 ppm C_2H_5Cl, 0.4 mol% C_2H_6, balance He; 5.3 bar; 513 K; catalyst mass = 0.027–0.082 g 6.9–35 wt% unpromoted Ag/α-Al_2O_3. Data acquired at 18 h on-stream after steady state rates were obtained.

shows that three catalysts (35S-3, 16.9S-1, and 31S-9) primarily containing Ag particles of sizes <100 nm have residuals >30% and thus deviate slightly from the parity line in Fig. 6 (b). Catalysts (35S-5, 35S-6, 35S-7, 35S-8) containing a large fraction of Ag particles with sizes >180 nm have much smaller residuals (<15%) implying that Gaussian model captures rate contributions from large particles better compared to the ones <100 nm.

Consider two catalysts: 35S-2 (Table 2) and mix-2 (Table 3) that have similar average particle sizes of 176.1 nm and 181.6 nm respectively but exhibit almost 2× differences in EO rates (35S-2 – 3.49 μmol g_{Ag}^{-1} s^{-1}, mix-2 – 1.79 μmol g_{Ag}^{-1} s^{-1}). A description based on average particle size (Eq. (2)) would predict similar rates (35S-2 – 2.66 μmol g_{Ag}^{-1} s^{-1}, mix-2 – 2.46 μmol g_{Ag}^{-1} s^{-1}) for the two samples as it lacks information about the breadth of the distribution as well as the population of different particle sizes that constitute the distribution. The distribution of surface area per gram for the two catalysts (Fig. 7) not only reveals the broader span of particle sizes in mix-2 but also the higher fraction of particles between 140 nm and 180 nm in 35S-2 that contributes to its higher observed EO rate which is captured by the Gaussian rate-function model (Fig. 6 (a, b)).

We can classify the samples listed in Table 2 in three categories based on the measured EO rates and Ag particle size distribution: (i) 6.9 wt% and 9.9 wt% catalysts containing small particle sizes between 40 and 80 nm that have intermediate EO rates ∼ 2–3 μmol g_{Ag}^{-1} s^{-1} (ii) 16.9 wt% and 35 wt% catalysts with intermediate particle sizes between 80 and 140 nm that have high EO rates ∼4–5 μmol g_{Ag}^{-1} s^{-1} (iii) 35 wt% catalysts with large particle sizes between 180 and 300 nm that have low EO rates ∼0.5–1 μmol g_{Ag}^{-1} s^{-1}. The surface area histograms for two or three catalysts in each of these three categories, are overlayed in Fig. 8 (a, b, c).

The Gaussian rate function model (Fig. 6 (a)) suggests that very small (5–50 nm) and very large Ag particles (>250 nm) have low

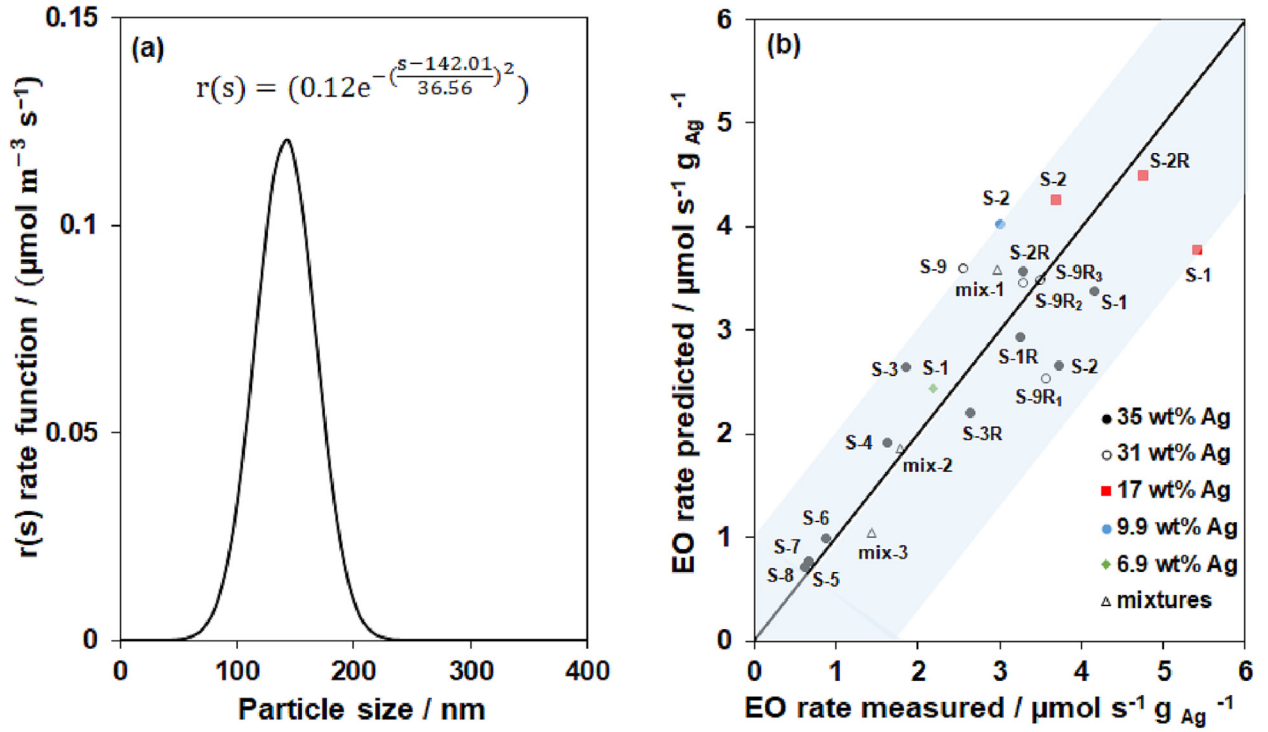

Fig. 6. (a) Variation of the fitted rate function model with particle size (b) Parity plot comparing the measured EO rates with rates predicted by the Gaussian rate function model (Eq.4). Each data point is associated with a catalyst having Ag weight loading as mentioned in the legend and the catalyst nomenclature from Tables 2 and 3 was used here with an additional letter 'R' to represent a replicate experiment.

Table 4
Fitted values for the parameters of the Gaussian rate function model described by Eq. (4). Uncertainties represent the 95% confidence intervals generated by Athena Visual studio.

Parameter	Value
a	$1.21 \times 10^{-1} \pm 1.33 \times 10^{-1}$ μmol m^{-3} g_{Ag}^{-1} s^{-1}
b	$-1.42 \times 10^{2} \pm 2.34 \times 10^{1}$ nm
c	$3.66 \times 10^{1} \pm 4.81 \times 10^{1}$ nm

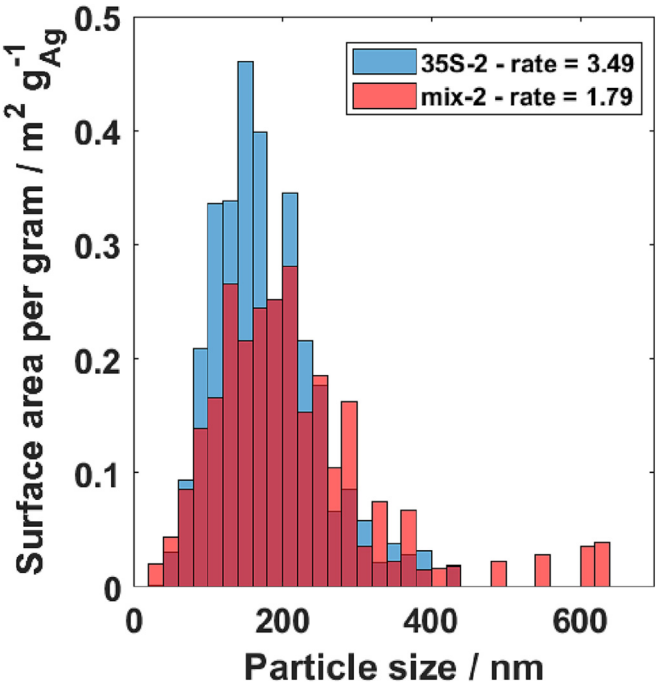

Fig. 7. A histogram of exposed surface area per gram as a function of particle size for two catalysts 35S-2 and mix-2 (Tables 2 and 3). The unit for rates of two catalysts mentioned in the legend is μmol g_{Ag}^{-1} s^{-1}.

reactivity whereas Ag particles ~130–150 nm have optimal reactivity. Particle size dependent rates in ethylene epoxidation catalysis have been rationalized variously as arising due to:

(i) Geometric factors such as exposed crystal facets (e.g., Ag (1 1 0), Ag(1 1 1)) or different coordination environment of sites exposed by metal clusters: Steady state turnover rates for EO and CO_2 production measured by Campbell [23] over Ag (1 1 1) and Ag (1 1 0) single crystal surfaces at 20 torr C_2H_4 and 150 torr O_2 at 490 K varied <2× implying that variation in epoxidation rates of ~10× that we observe (Fig. 3(a)) cannot be solely explained by differences in exposed facets with particle size.

(ii) Electronic factors like metal work function/ binding energy or charge transfer between metal and support: Bukthiyarov et al. [24] have correlated the changes in ethylene consumption rates (0.2 to 5 μmol $m_{catalyst\ (BET)}^{-2}$ s^{-1}) with Ag particle size (20 to 100 nm) to corresponding changes in Ag $3d_{5/2}$ binding energies from 368.4 eV to 367.9 eV thus revealing electronic changes in Ag particles with increasing size.

(iii) Particle morphology: Christopher and Linic [9] measured different ethylene epoxidation rates over Ag/α-Al_2O_3 catalysts having different shapes (100 nm nanospheres – 1.9×10^{-2} mmol g_{Ag}^{-1} min^{-1}, 90 nm nanocubes – 2.3×10^{-3} mmol g_{Ag}^{-1} min^{-1}, and 75 nm nanowires – 1.2×10^{-2} mmol g_{Ag}^{-1} min^{-1}) at 510 K and 1 atm pressure suggesting a possible role of Ag particle morphology in inducing particle size effects.

Particle size effects manifest as changes in rate/equilibrium constants for elementary steps involved in ethylene epoxidation. Two plausible rate limiting steps have been proposed by Stegelmann et al. [25] based on microkinetic modeling studies: (i) adsorption of oxygen over silver and (ii) surface reaction between adsorbed ethylene and adsorbed oxygen. Lamoth et al. [26] treated a 5 wt% Ag/SiO_2 catalyst containing sub-30 nm Ag particles and a 13.7 wt% Ag/α-Al_2O_3 catalyst containing Ag particles between 20 and 250 nm under 1.67 cm^3 s^{-1} of 25% O_2/Ar at 1 bar and 483 K for 12 h prior to thermal desorption (heating rate of 25 K min^{-1} up to 973 K) under vacuum and found that the amount of oxygen desorbed was ~17× higher in case of 5 wt% Ag/SiO_2 (293 μmol 'O' g_{Ag}^{-1}) compared to the 13.7 wt% Ag/α-Al_2O_3 (17 μmol 'O' g_{Ag}^{-1}) catalyst. Moreover, the temperature of the maximum in oxygen desorption was 638 K for 5 wt% Ag/SiO_2 compared to 440 K for 13.7 wt% Ag/α-Al_2O_3 which the authors attributed to stronger Ag-O interactions in smaller Ag particles. Li et al. [27] used DFT calculations and scaling relations to show that high O-binding energy (>1 eV) can increase activation barriers for the surface reaction of oxygen with ethylene despite facile O_2 adsorption which is a plausible explanation for low rates over small Ag particles. Other factors such as changes in chlorine coverage or coverages of other surface intermediates with particle size could also play a role in inducing particle size effects. An extremum in epoxidation rate with particle size (~130–150 nm) is likely caused by a combination of such factors. While the underlying cause to the observed particle size effect remains a topic of study, what is evident from the work we report is that the electronic and geometric attributes that contribute to these size effects should be associated with the Ag particle size distribution in ethylene epoxidation catalysis and these attributes are not captured by models that correlate measured rates to average particle size.

3.4. Determination of optimal Ag particle size for ethylene epoxidation

The rate function model, that defines rate as the product of the rate function and exposed surface area per gram (Eq. (3)), can be used to determine the optimal Ag particle size that maximizes epoxidation rates. This is different from the size corresponding to the peak in the Gaussian rate function (142 nm) as shown in Fig. 6 (a). Hypothetically, we could generate catalyst samples containing Ag particles of identical sizes between 5 and 400 nm in intervals of 1 nm. At a given particle size s = D, the epoxidation rate is given by the product of the rate function r(D) and the exposed surface area per gram (A(D)) calculated using Eq. (3) that varies with particle size as shown in Fig. 9. Expressing the rate as a continuous function of particle size in the form of a Gaussian function allows us to calculate ~140 nm as the optimal size that maximizes epoxidation rate with EO selectivities >76%. An Ag/Al_2O_3 sample with a narrow size distribution centered around 140 nm would thus yield ~10× higher rates per gram compared to distributions centered around very small (~30 nm) or very large Ag particle sizes

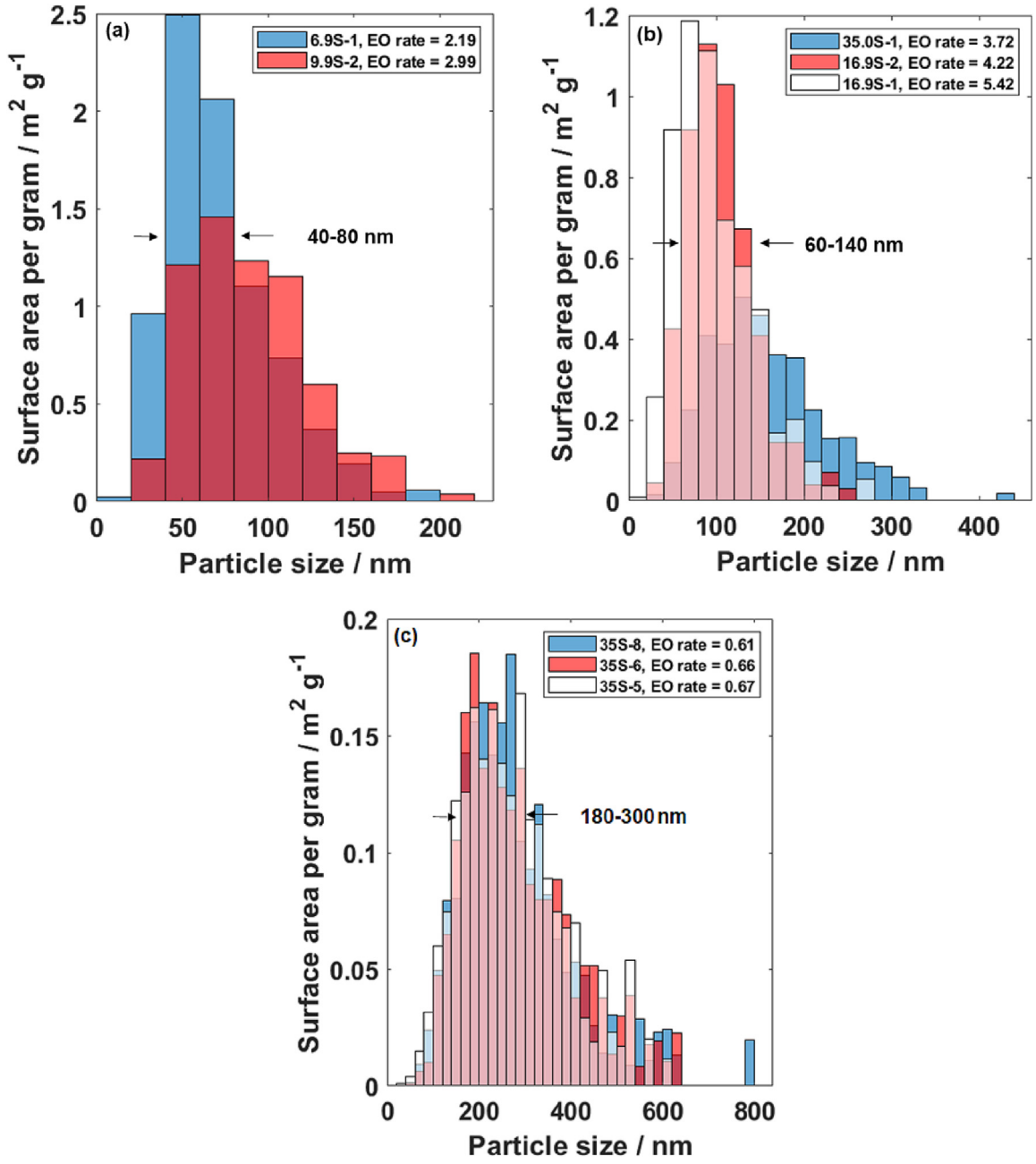

Fig. 8. A histogram of exposed surface area per gram as a function of particle size for (a) 6.9S-1, 9.9S-2 (b) 35S-1, 16.9S-1, 16.9S-2 (c) 35S-5, 35S-6, 35S-8 (refer to Table 2). The unit for rates for all catalysts mentioned in the legend is μmol g_{Ag}^{-1} s^{-1}.

(∼250 nm) under the conditions of our study. Notably, a recent study from Egelske et al. [10] showed that Ag particles <100 nm exhibit a significantly lower EO selectivity of 58% compared to Ag particles >100 nm (EO selectivity ∼ 73%) which the authors correlated with increased Ag sintering and carbon fouling over small Ag particles which reaffirms why large Ag particles (∼130–150 nm) are beneficial in ethylene epoxidation catalysis under differential ethylene conversions as they exhibit high EO rates and EO selectivity. Under integral ethylene conversions effects such as gradients in chlorine coverage and changes in ethylene and oxygen reaction orders for EO formation along the reactor bed can impact ethylene epoxidation rates and selectivity [28] which may result in a different optimal Ag particle size distribution.

4. Conclusions

The effects of Ag particle size on ethylene epoxidation rates were studied over 6.9–35 wt% Ag/α-Al_2O_3 catalysts with varying particle size distributions. EO rates increase with average particle size until ∼110 nm before decreasing with size. Particle size effects were better described when the Ag surface area (per gram)

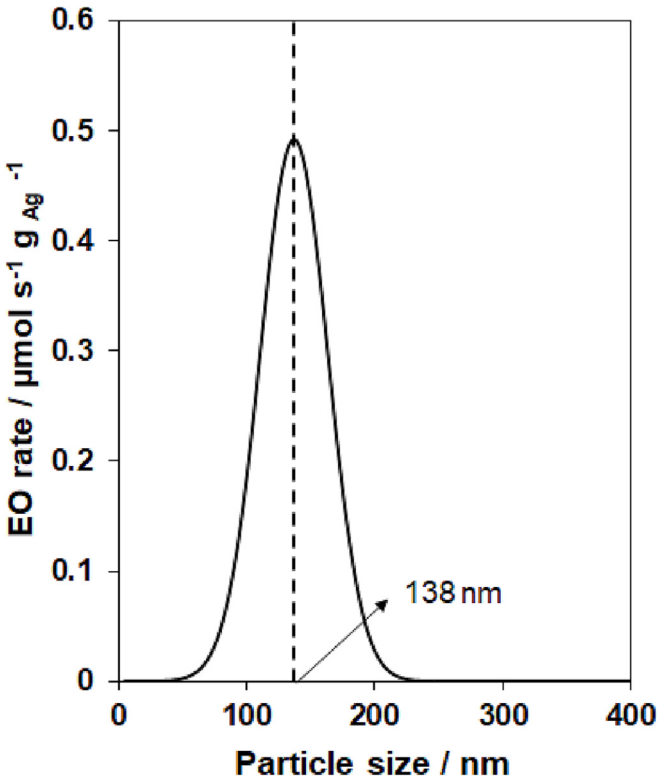

Fig. 9. EO rates as a function of particle size calculated using the product of the rate function and exposed surface area per gram (Eq. (3)) at each particle size between 5 and 400 nm.

distributions of spent Ag/α-Al_2O_3 catalysts were correlated to the observed EO rates via a Gaussian particle size-dependent rate function over a wide range of particle sizes (5–400 nm) than a description based on average particle size as the latter omits details related to the breadth of the distribution and the population of particles of different sizes. The Gaussian rate function model reveals that very small Ag particles (5–50 nm) and large Ag particles (>250 nm) exhibit low EO rates which can plausibly be explained based on changes in the binding energy of oxygen and other surface intermediates with silver particle size. The model also suggests optimal particle size distributions of Ag/α-Al_2O_3 centered around (∼140 nm) will facilitate high EO rates (>4 μmol g_{Ag}^{-1} s^{-1}).

Data availability

Data will be made available on request.

Declaration of Competing Interest

The authors declare that they have no known competing financial interests or personal relationships that could have appeared to influence the work reported in this paper.

Acknowledgements

Parts of this work were carried out in the Characterization Facility, University of Minnesota, which receives partial support from the NSF through the MRSEC and the NNCI programs. The authors acknowledge Dr. Xinyu Li for assistance with XRD analysis, Prof. David Poerschke and Mr. Atharva Chikhalikar for helping out with heat treatment of γ-Al_2O_3, Dr. Christopher Ho at Dow Inc., for assistance with parameter estimation in Athena Visual Studio and Dr. Victor Sussman and Dr. Daniel Hickman at Dow Inc., for helpful technical discussions. The authors gratefully acknowledge funding support from Dow through the University Partnership Initiative.

Appendix A. Supplementary data

Supplementary data to this article can be found online at https://doi.org/10.1016/j.jcat.2023.02.008.

References

[1] S. Overbury, V. Schwartz, D. Mullins, W. Yan, S. Dai, Evaluation of the Au Size Effect: CO Oxidation Catalyzed by Au/TiO_2, J. Catal. 241 (1) (2006) 56–65, https://doi.org/10.1016/j.jcat.2006.04.018.
[2] M. Du, D. Sun, H. Yang, J. Huang, X. Jing, T. Odoom-Wubah, H. Wang, L. Jia, Q. Li, Influence of Au Particle Size on Au/TiO_2 Catalysts for CO Oxidation, J. Phys. Chem. C 118 (33) (2014) 19150–19157, https://doi.org/10.1021/jp504681f.
[3] J.P. den Breejen, P.B. Radstake, G.L. Bezemer, J.H. Bitter, V. Frøseth, A. Holmen, K.P. de Jong, On the Origin of the Cobalt Particle Size Effects in Fischer–Tropsch Catalysis, J. Am. Chem. Soc. 131 (20) (2009) 7197–7203, https://doi.org/10.1021/ja901006x.
[4] Z. Wang, S. Skiles, F. Yang, Z. Yan, D.W. Goodman, Particle Size Effects in Fischer-Tropsch Synthesis by Cobalt, Catal. Today 181 (1) (2012) 75–81, https://doi.org/10.1016/j.cattod.2011.06.021.
[5] J.E. van den Reijen, S. Kanungo, T.A.J. Welling, M. Versluijs-Helder, T.A. Nijhuis, K.P. de Jong, P.E. de Jongh, Preparation and Particle Size Effects of Ag/α-Al_2O_3 Catalysts for Ethylene Epoxidation, J. Catal. 356 (2017) 65–74, https://doi.org/10.1016/j.jcat.2017.10.001.
[6] J.K. Lee, X.E. Verykios, R. Pitchai, Support and Crystallite Size Effects in Ethylene Oxidation Catalysis, Appl. Catal. 50 (1) (1989) 171–188, https://doi.org/10.1016/S0166-9834(00)80834-9.
[7] S.N. Goncharova, E.A. Paukshtis, B.S. Bal'zhinimaev, Size Effects in Ethylene Oxidation on Silver Catalysts. Influence of Support and Cs Promoter, Applied Catalysis A: General 126 (1) (1995) 67–84, https://doi.org/10.1016/0926-860X(95)00036-4.
[8] A.J.F. van Hoof, E.A.R. Hermans, A.P. van Bavel, H. Friedrich, E.J.M. Hensen, Structure Sensitivity of Silver-Catalyzed Ethylene Epoxidation, ACS Catal. 9 (11) (2019) 9829–9839, https://doi.org/10.1021/acscatal.9b02720.
[9] P. Christopher, S. Linic, Shape- and Size-Specific Chemistry of Ag Nanostructures in Catalytic Ethylene Epoxidation, ChemCatChem 2 (1) (2010) 78–83, https://doi.org/10.1002/cctc.200900231.
[10] B.T. Egelske, W. Xiong, H. Zhou, J.R. Monnier, Effects of the Method of Active Site Characterization for Determining Structure-Sensitivity in Ag-Catalyzed Ethylene Epoxidation, J. Catal. 410 (2022) 221–235, https://doi.org/10.1016/j.jcat.2022.03.021.
[11] J.C. Wu, P. Harriott, The Effect of Crystallite Size on the Activity and Selectivity of Silver Catalysts, J. Catal. 39 (3) (1975) 395–402, https://doi.org/10.1016/0021-9517(75)90306-1.
[12] X.E. Verykios, F.P. Stein, R.W. Coughlin, Influence of Metal Crystallite Size and Morphology on Selectivity and Activity of Ethylene Oxidation Catalyzed by Supported Silver, J. Catal. 66 (2) (1980) 368–382, https://doi.org/10.1016/0021-9517(80)90040-8.
[13] S. Cheng, A. Clearfield, Oxidation of Ethylene Catalyzed by Silver Supported on Zirconium Phosphate: Particle Size and Support Effect, J. Catal. 94 (2) (1985) 455–467, https://doi.org/10.1016/0021-9517(85)90210-6.
[14] J. Lu, J. Bravosuarez, A. Takahashi, M. Haruta, S. Oyama, In Situ UV–Vis Studies of the Effect of Particle Size on the Epoxidation of Ethylene and Propylene on Supported Silver Catalysts with Molecular Oxygen, J. Catal. 232 (1) (2005) 85–95, https://doi.org/10.1016/j.jcat.2005.02.013.
[15] A.J.F. van Hoof, I.A.W. Filot, H. Friedrich, E.J.M. Hensen, Reversible Restructuring of Silver Particles during Ethylene Epoxidation, ACS Catal. 8 (12) (2018) 11794–11800, https://doi.org/10.1021/acscatal.8b03331.
[16] A.J.F. van Hoof, R.C.J. van der Poll, H. Friedrich, E.J.M. Hensen, Dynamics of Silver Particles during Ethylene Epoxidation, Appl Catal B 272 (2020), https://doi.org/10.1016/j.apcatb.2020.118983.
[17] P.H. Keijzer, J.E. van den Reijen, C.J. Keijzer, K.P. de Jong, P.E. de Jongh, Influence of Atmosphere, Interparticle Distance and Support on the Stability of Silver on α-Alumina for Ethylene Epoxidation, J. Catal. 405 (2022) 534–544, https://doi.org/10.1016/j.jcat.2021.11.016.
[18] J.C. Dellamorte, J. Lauterbach, M.A. Barteau, Effect of Preparation Conditions on Ag Catalysts for Ethylene Epoxidation, Top. Catal. 53 (1–2) (2010) 13–18, https://doi.org/10.1007/s11244-009-9440-9.
[19] R.S. Weber, Lies, Damned Lies, and Turnover Rates, J. Catal. 404 (2021) 925–928, https://doi.org/10.1016/j.jcat.2021.06.024.
[20] M. Peuckert, T. Yoneda, R.A.D. Betta, M. Boudart, Oxygen Reduction on Small Supported Platinum Particles, J. Electrochem. Soc. 133 (5) (1986) 944–947, https://doi.org/10.1149/1.2108769.
[21] J.H. Miller, A. Joshi, X. Li, A. Bhan, Catalytic Degradation of Ethylene Oxide over Ag/α-Al_2O_3, J. Catal. 389 (2020) 714–720, https://doi.org/10.1016/j.jcat.2020.07.008.
[22] D.A. Hickman, J.C. Degenstein, F.H. Ribeiro, Fundamental Principles of Laboratory Fixed Bed Reactor Design, Curr. Opin. Chem. Eng. 13 (2016) 1–9, https://doi.org/10.1016/j.coche.2016.07.002.

[23] C. Campbell, The Selective Epoxidation of Ethylene Catalyzed by Ag(111): A Comparison with Ag(110), J. Catal. 94 (2) (1985) 436–444, https://doi.org/10.1016/0021-9517(85)90208-8.
[24] V.I. Bukhtiyarov, I.P. Prosvirin, R.I. Kvon, S.N. Goncharova, B.S. Bal'zhinimaev, XPS Study of the Size Effect in Ethene Epoxidation on Supported Silver Catalysts, Journal of the Chemical Society, Faraday Transactions 93 (13) (1997) 2323–2329, https://doi.org/10.1039/a608414a.
[25] C. Stegelmann, N.C. Schiødt, C.T. Campbell, P. Stoltze, Microkinetic Modeling of Ethylene Oxidation over Silver, J. Catal. 221 (2) (2004) 630–649, https://doi.org/10.1016/j.jcat.2003.10.004.
[26] M. Lamoth, T. Jones, M. Plodinec, A. Machoke, S. Wrabetz, M. Krämer, A. Karpov, F. Rosowski, S. Piccinin, R. Schlögl, E. Frei, Nanocatalysts Unravel the Selective State of Ag, ChemCatChem 12 (11) (2020) 2977–2988, https://doi.org/10.1002/cctc.202000035.
[27] H. Li, A. Cao, J.K. Nørskov, Understanding Trends in Ethylene Epoxidation on Group IB Metals, ACS Catal. 11 (19) (2021) 12052–12057, https://doi.org/10.1021/acscatal.1c03094.
[28] K.R. Iyer, A. Bhan, Interdependencies Among Ethylene Oxidation and Chlorine Moderation Catalytic Cycles Over Promoted Ag/α-Al_2O_3 Catalysts, ACS Catal. 11 (24) (2021) 14864–14876, https://doi.org/10.1021/acscatal.1c03493.